# An Important Double Bond: Effects of 22:5n-6 vs. 22:6n-3 on Visual Signal Transduction


Drake C. Mitchell[1] & Shui-Lin Niu[2]

[1]Department of Physics, Portland State University; [2]Laboratory of Membrane Biochemistry & Biophysics, N. I. A. A. A., N.I.H.



## ABSTRACT

In a normal, healthy retinal rod outer segment 40% to 50% of the phospholipid acyl chains consist of docosahexaenoic acid (DHA, 22:6n-3). Diets that are deficient in n-3, or ω-3, fatty acids lead to the replacement of 22:6n-3 with 22:5n6. Dietary n-3 deficiency leads to a spectrum of developmental disorders associated with learning, memory, intelligence, and visual function. We examined rhodopsin, transducin ($G_t$) and phosphodiesterase (PDE) function and acyl chain packing in large unilamellar proteoliposomes consisting of phosphatidylcholines with *sn-1* = 18:0, and *sn-2* = 22:6n-3, 22:5n-6 or 22:5n-3. Rhodopsin activation and binding to $G_t$ was assayed with steady-state and time-resolved UV/vis spectroscopy, acyl chain packing was assessed via time-resolved fluorescence of diphenylhexatriene (DPH) and PDE activity was determined from the change in pH due to hydrolysis of cyclic GMP. The motion of DPH in the membrane was slower in 22:5n-6 than in 22:6n-3 and overall acyl chain packing was more constrained. The most significant structural difference between the 22:5n-6 containing bilayer and bilayers containing both n-3 polyunsaturates was in the bilayer mid plane where 22:5n-6 produced much higher DPH orientational order. At physiological temperature the formation of both the active metarhodopsin II conformation (MII) and the MII-$G_t$ complex was much slower in 18:0,22:5n-6 PC than in 18:0,22:6n-3 PC and the equilibrium amount of MII formed was 50% higher in 18:0,22:6n-3 PC. In 18:0,22:5n-6 PC PDE activity at a physiologically relevant level of rhodopsin activation is only about 60% of that observed in either 18:0,22:6n-3 PC or 18:0,22:5n-3 PC. Taken together, these results demonstrate that the subtle change in bond configuration from 22:6n-3 to 22:5n-6 produces more structured acyl chain packing in the bilayer midplane, leading to delayed and reduced MII–$G_t$ interaction and PDE function.


## INTRODUCTION

Visual signal transduction begins when light is absorbed by rhodopsin, as shown in FIGURE 1, below. A metastable, dynamic equilibrium between two conformational states of photoexcited rhodopsin, designated MI and MII, is established within a few milliseconds of photon absorption. MII is the conformation which binds and activates the visual G protein, transducin ($G_t$), as shown in step 1, below. Transducin, $G_t$, is a peripheral membrane protein (MW = 80,000) with an $\alpha\beta\gamma$ subunit composition, Binding of $G_t$ by MII catalyzes the exchange of GDP for GTP, which destabilizes the trimer, and the visual signal is carried from rhodopsin to a phosphodiesterase (PDE) by $G_\alpha$-GTP, step 2, below. Each activated PDE hydrolyzes several hundred molecules of cGMP (step 3, below) which results in closure of cGMP sensitive Na+ channels in the cell membrane.

FIGURE 1

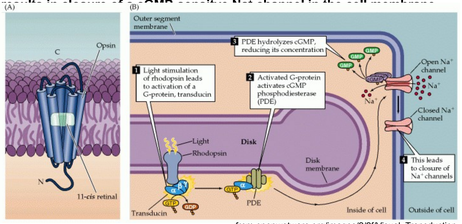


from openwetware.org/images/2/2f/Visual_Transduction

**Left Panel**: Rhodopsin in the disk membrane.

**Right Panel**: Visual signal transduction in the rod outer segment from rho to $G_t$ to PDE to $Na^+$ channel.

In a normal, healthy rod outer segment 40% to 50% of the phospholipid acyl chains consist of docosahexaenoic acid (DHA, 22:6n3). Diets that are deficient in n3, or ω-3, fatty acids lead to the replacement of 22:6n3 with 22:5n6. Such diets also lead to a spectrum of developmental disorders associated with learning, memory, intelligence, and visual function (1). We examined membrane physical properties and rhodopsin, transducin and PDE function in membranes consisting of phosphatidylcholines with *sn-1* = 18:0, and *sn-2* = 22:6n3 or 22:5n6 or 22:5n3.

1.Membrane physical properties were assessed with time-resolved fluorescence lifetime and anisotropy decay measurements of the fluorescent membrane probe DPH (diphenylheaxtriene).

2.Rhodopsin conformation change was assessed in terms of the MI-MII equilibrium.

3.The kinetics of MII and MII• $G_t$ formation were measured directly using flash photolysis. In the absence of GTP MII• $G_t$ is stable, and has the same absorption spectrum as unbound MII.

4.PDE activity was directly measured in the presence of rhodopsin and $G_t$ via the change in pH due to cGMP hydrolysis.

## METHODS

*Sample preparation* - Rod outer segments (ROS) were isolated from frozen retinas and rhodopsin was purified using a con-A affinity column. Transducin and phosphodiesterase (PDE) were prepared together as a hypotonic extract. Rhodopsin-containing unilamellar vesicles were prepared using a rapid dilution method with lipid to rhodopsin ratio of 100:1. The lipid to rhodopsin ratio for each preparation was determined by independent lipid and protein assays. Samples for equilibrium and kinetic measurements contained 7.5 μ M rhodopsin in reconstituted vesicles incubated with or without transducin (1.5 μ M) for 3 hours on ice in pH 7.5 TBS buffer before assays.

*MI-MII equilibrium measurements* – MI-MII equilibrium were measured by acquiring a series of four UV/vis absorption spectra as described. MI and MII were de-convoluted from the difference spectra using nonlinear least square fit and used to calculate the K of MI-MII equilibrium (2).

*Flash photolysis measurements* – Kinetics of MII and MII·G formation were measured using a flash photolysis system of our own design to measure the transient absorption at 380 nm following rapid excitation at 500nm (3). The change in absorbance at 380 nm in the absence of $G_t$ was analyzed in terms of the square photoreaction model of Kliger and coworkers (4). Kinetic traces of $G_t$-containing samples show both MII and MII-$G_t$ complex formation. MII were analyzed with the square model plus an additonal exponential term.

*Fluorescence Measurements* Lifetime and differential polarization measurements were performed with a K2 multifrequency cross-correlation phase fluorometer (ISS). Both total intensity decay and differential polarization measurements were repeated at each temperature with each bilayer composition a minimum of three times. Total fluorescence intensity decays were analyzed in terms of the sum of 3 discrete exponential decays. All anisotropy decay data were analyzed using the Brownian rotational diffusion model which yields the order parameters <P2> and <P4>. The results of the BRD model-based analysis were interpreted in terms of an angular distribution function which is symmetric about θ = π /2 (5)$I(\theta) = N^{-1}\exp[\lambda_2 P_2(\cos\theta) + \lambda_4 P_4(\cos\theta)]$ (Equation 1) where $\lambda_2$ and $\lambda_4$ are constants determined by simultaneous solution of equations for <P2> and <P4> and N is the normalization constant determined according to $N = \int_0 \sin(\theta)\exp[\lambda_2 P_2(\cos\theta) + \lambda_4 P_4(\cos\theta)]d\theta$ (Equation 2)

*PDE Activity* - PDE activity was assayed using a real-time pH method (6) with the following modifications. A high sensitivity pH meter with built-in temperature compensation coupled to a micro-electrode was used to monitor pH. The signal output from the pH meter was acquired by a computer through a 12-bit A/D board operated at 1kHz rate. Samples that contained 5 μ M rhodopsin , $G_t$ and PDE, 50 μ M GTP and 1 mM cGMP in TBS buffer (pH 8.0) were pre-incubated at 37 ° C in a thermo-regulated micro-cuvette in the dark for 10 minutes. A set of 20 data points was collected as the baseline activity prior to sample activation by a flash lamp synchronized by the computer. The light intensity was attenuated using neutral density filters to vary the level of rhodopsin activation in samples, which was determined by rhodopsin concentrations before and after light exposure. The PDE activity is obtained from the shift in pH and is expressed as cGMP hydrolyzed(mM)/sec.

## QUESTIONS

1. Are there differences in ensemble acyl chain packing, as detected by the motion of DPH, in bilayers consisting of 18:0,22:6n3 PC, 18:0,22:5n6 PC, and 18:0,22:5n3 PC?
2. The kinetics of receptor-$G_t$ complex formation results from the diffusion of both proteins in the plane of the membrane. To what extent is this kinetics subject to changes in the specific bond configuration of 22-carbon fatty acids at the *sn-2* position?
3. Phosphodiesterase (PDE) activity results from the integrated response of photo-activated rhodopsin and $G_t$. Is this response modulated by the relatively subtle change in membrane composition which results from substitution of 22:5n6 for 22:6n3 at the *sn-2* position?

## RESULTS

### Membrane Properties

FIGURE 2

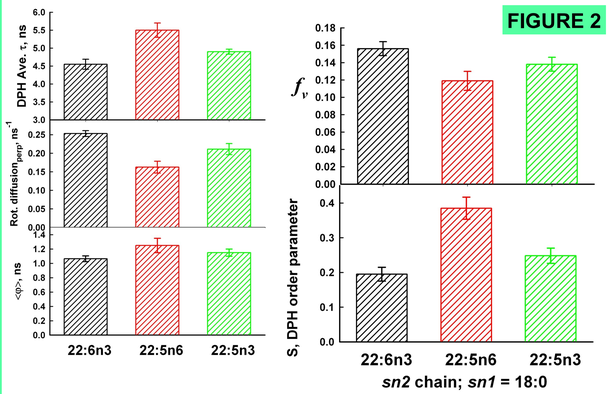


**Left: (Top Panel)** The intensity-weighted fl. lifetime of DPH is significantly longer in the 22:5n6 lipid than in the two n3 lipids, showing that water penetration is highest in the 22:5n6 membrane. **(Bottom 2 Panels)** Both parameters report DPH rotational motion; $D_{perp}$ is from the BRD analysis and φis from the empirical, model-free analysis. Both parameters show that DPH rotates significantly slower in 22:5n6 than in the 2 n3 lipids.

**Right:** These two parameters report DPH euilibrium order, $f_v$ is a disorder parameter from the BRD analysis and S is an order parameter from the empirical, model-free analysis. Both parameters show that DPH is most ordered in 22:5n6, while it has about the same degree of disorder in the two n3 lipids.

FIGURE 3

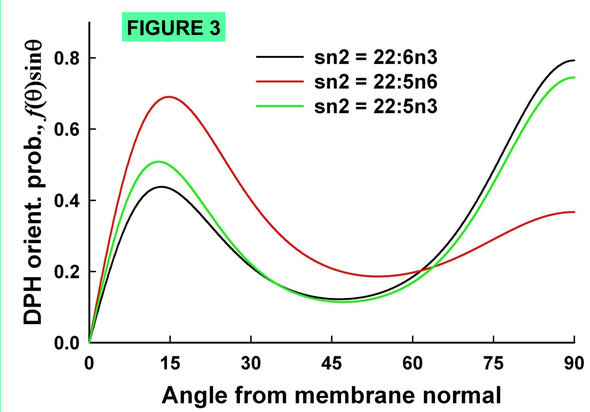


Plots of the DPH orientational probability distributions obtained from the BRD analysis of fluorescence anisotropy decays (see Equation 1 in METHODS). The curves for the two n3 lipids are very similar, both showing a high probability of DPH at 90° from the membrane normal, presumably in the bilayer midplane. The curve for 22:5n6 shows that DPH in this bilayer is about 50% less likely to be in the bilayer midplane. These curves show that acyl chain packing in the n6 bilayer is more constrained than in the n3 bilayers throughout the depth of the bilayer.

## Rhodopsin Function

FIGURE 4

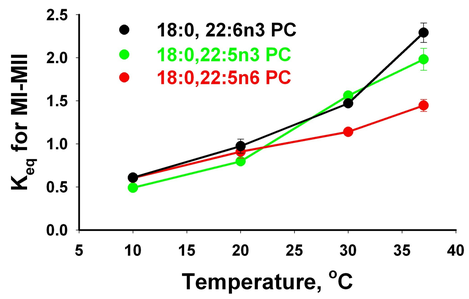


Effect of temperature on the MI – MII conformational equilibrium of photo-activated rhodopsin. At lower temperatures the extent of MII formation is the same in all 3 bilayers, but at physiological temperature the amount of MII formed is significantly higher in the two n3 lipids.

FIGURE 5

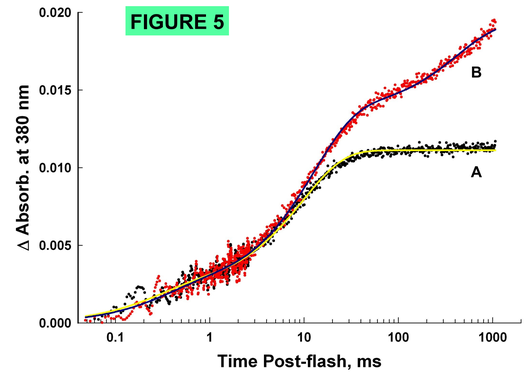


Examples of flash photolysis measurements of MII formation in the absence (A) and presence (B) of $G_t$ at 20°C, pH7.0. Trace B was acquired in the absence of GTP, thus it shows the formation of both MII and the MII• $G_t$ complex. The smooth curve in A is the result of analysis in terms the square model, the smooth curve in B is from analysis with the square model plus an additional exponential term to account for MII – $G_t$ binding.

FIGURE 6

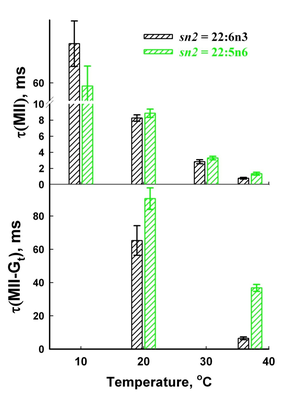


Summary of the kinetics of MII and MII• $G_t$ formation in 18:0,22:6n3 PC and 18:0,22:5n6 PC.

**Upper Panel:** The unimolecular reaction of MI to MII is faster in 22:6n3 at 30 and 37C, although the differences are relatively modest.

**Lower Panel:** At 37C the bimolecular reaction to form the MII• $G_t$ complex occurs ~5x slower in 22:5n6 compared to 22:6n3. The rate of this reaction is governed by lateral diffusion, thus the 22:5n6 membrane appears to dramatically slow protein lateral diffusion.

## PDE Activity

FIGURE 7

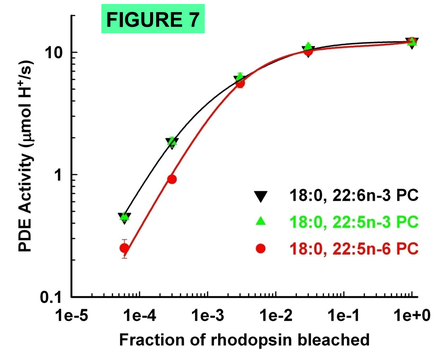


Dose-response curves showing the effect of increasing rhodopsin bleach on PDE activity. The convergence of the curves at bleach levels above ~ 0.5% indicates that at these saturating 'dose' levels all available cGMP is hydrolyzed. The only physiologically relevant bleach level in this series is the one at frac. bleach = 0.00006.

FIGURE 8

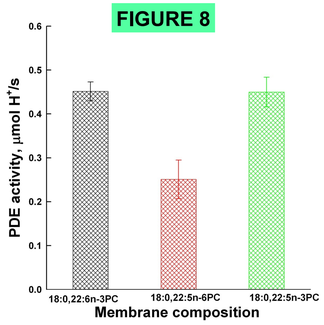


Comparison of PDE activity at the lowest bleach level (see Fig. 7, above). At this physiologically relevant level of rhodopsin stimulus PDE activity is identical in the two n3 lipids, while it is about 50% lower in 22:5n6.

## SUMMARY & CONCLUSIONS

1. The motion of DPH in the membrane is altered by the double bond configuration of a 22-carbon fatty acid at the sn-2 position, Fig. 2. Overall acyl chain packing, as quantified by S and $f_v$, is also altered, Fig. 2. However, the most significant difference between 22:5n6 and 22:6n3/22:5n3 is in the region of the bilayer profile that is disordered. The high DPH orientational probability for the n3's above 60° shows that the bilayer mid plane is much more disordered in these two bilayers, Fig. 3.
2. At physiological temperature less MII is formed, Fig. 4, and the formation of MII and MII-$G_t$ is much slower in 18:0,22:5n6 PC Fig. 6.
3. In 18:0,22:5n6 PC PDE activity at a physiological bleach level is only about 50% of that observed in either 18:0,22:6n3 PC or 18:0,22:5n3 PC, Fig. 7, Fig. 8.

Taken together, these results demonstrate that the subtle change in bond configuration from 22:6n3 to 22:5n6 produces more structured acyl chain packing in the bilayer midplane, leading to delayed and reduced MII – $G_t$ interaction and a slower rate of PDE function.

## REFERENCES


1. Salem, N. Jr. et al. (2001) Lipids 36:945-959.
2. Straume, M. Mitchell, D.C. ,Miller, J.L., and Litman, B.J. (1990) Biochemistry 29, 9135-9142.
3. Mitchell, D. C., Niu, S.L. and Litman, B.J. (2001) J. Biol. Chem. 46:42801-6.
4. Thorgeirsson, T.E., Lewis, J.W., Wallace-Williams, S.E. and Kliger, D.S. (1993) Biochemistry 32:13861-72.
5. Mitchell, D.C. and Litm,an, B.J. (1998) Biophys. J. 74:879-91.
6. Yee, R. & Liebman, P.A. (1978) *J. Biol. Chem.* 253, 8902-8909.